4A.3 TTUKa Radar Observations of Horizontal Vorticity Maxima Associated with Rear Flank Downdrafts and Gust Fronts

Christopher C. Weiss*
Texas Tech University, Lubbock, Texas

Patrick S. Skinner, Anthony E. Reinhart
Texas Tech University, Lubbock, Texas

1. INTRODUCTION

Horizontal vorticity in the storm-scale environment has long been attributed to the genesis and intensification of low- and mid-level mesocyclones and tornadoes (e.g., Rotunno and Klemp 1985; Davies-Jones and Brooks 1993; Adlerman et al. 1999; Davies-Jones 2000; Markowski et al. 2012a,b; Beck and Weiss 2013). Mechanisms pertaining to baroclinic solenoids, for example, produce horizontal vorticity; air parcels inbound to the low-level mesocyclone and tornado can acquire this sense of vorticity and tilt this component into the vertical upon interaction with the storm-scale downdraft/updraft interface.

The descending reflectivity core (DRC), initially described by Rasmussen et al. (2006), is an example of such a baroclinic mechanism, whereby local maxima in reflectivity (i.e., hydrometeor concentration, size and, therefore, fall speed) within the body of the hook echo region are observed to occur prior to the genesis of tornadoes (some significant) in a number of cases. Recent investigations (e.g., Kennedy et al. 2007; Markowski et al. 2008; Byko et al. 2009; Markowski et al. 2012a,b) have further suggested the presence of DRCs prior to the genesis of tornadoes in certain cases.

Compared to the number of numerical representations, there is a severe paucity of observations of horizontal vorticity within supercell thunderstorms. Particularly for the cases of such vorticity attributed to storm-scale heterogeneity (e.g., gust fronts leading the forward and rear flank downdrafts, DRCs), the authors are unaware of observations of such features that have been documented with high-frequency Doppler radar, which has motivated this targeted study using the Texas Tech Ka-band Doppler radars. (Details of the systems are documented by Weiss et al. (2011), with note of a recent upgrade to a 1.82-m diameter reflector on both platforms, permitting an angular beamwidth of 0.33 deg.)

* *Corresponding author address: Christopher C. Weiss, Texas Tech University, Atmospheric Science Group, Department of Geosciences, Lubbock, TX, 79409; e-mail: Chris.Weiss@ttu.edu*

2. DATA ANALYSIS

Data from both the TTUKa radar and Shared Mobile Atmospheric Research and Training Radars (SMART-R) are used in this study. As both cases discussed are from the second Verification of the Origin of Rotation in Tornadoes Experiment (VORTEX2), all radar data are obtainable from the VORTEX2 field catalog at: http://www.eol.ucar.edu/projects/vortex2/ Using SOLOII, all data are thresholded according to the returned power (in such cases where this moment is missing, reflectivity is used in its place), and dealiased. SOLOII and the Unidata Integrated Data Viewer are both used to produce the images presented in this paper.

As only single Doppler data are available for both cases, horizontal vorticity calculations in this paper are inferred from the assumption of Rankine vortex structure, where:

$$\eta_\theta = \frac{2}{r}\frac{\partial V_r}{\partial \phi} \quad (1)$$

where V_r is the radial velocity, r is the range and ϕ is the elevation angle.

3. REAR FLANK GUST FRONT CASE – 12 MAY 2010, WILLOW, OK

On 12 May 2010, VORTEX2 teams collected data on target storms in southwestern Oklahoma. Near 0000 UTC (13 May 2010), observations were focused on a non-tornadic HP supercell located near Willow, OK (Fig. 1), the updraft of which was in close proximity to a number of neighboring updrafts.

One TTUKa radar (TTUKa-1) deployed ahead of this target and performed a rapid sequence of RHI scans from 2352-0003 UTC. The plane of these scans was initially just to the north of the northward-surging rear flank gust front

(RFGF), providing an opportunity to assess the vertical structure of the RFGF boundary.

The RHI at ~2358 UTC, oriented at 265 degrees (north-relative) and positioned 1.2 km north of the apex of the RFGF, clearly identifies the leading edge of heavy precipitation that attenuates the 35 GHz signal at approximately 9.5 km range (Fig. 2). This precipitation lies behind the outflow boundary, the leading edge of which is identified near the surface at 7.5 km range and is sharply sloped rearward with height. However, at and above 2 km AGL, the maximum in reflectivity becomes collocated with the discontinuity in radial velocity. Further considering that the path-integrated reflectivity is markedly decreased at these higher elevations, the reflectivity maximum at these levels appears to truly depict a confluent boundary (rather than the just the leading portion of an attenuated signal). As such, the forward (eastward) tilt of the boundary with height is a marked difference from that associated with the density current below 2 km AGL.

Approaching 2359 UTC, at a position within 1 km of the RGFG apex, the structure of the boundary above 2 km AGL fragments considerably with a rather discontinuous eastward propagation evident (Fig. 3). At this point, the boundary shows first signs of inflections, which correspond well with areas of weak vertical shear in radial velocity.

By 0000 UTC, as the RHI plane begins to cut across the position of the RFGF, concentrated areas of horizontal vorticity O~10^{-1} s^{-1}, likely Kelvin-Helmholtz (KH) billows, develop along the vertical wave pattern (Fig. 4) and are coincident with a surge of inbound velocity behind the RFGF interface. Initial spacing of these vortices in the vertical is approximately 500-750 m. These vortices ascend along the boundary over the remaining 120 s of the deployment as the boundary transitions from a forward (eastward) slope to a rearward (westward) slope, more inline with the rearward density current structure below. Through this transition, the generation of new KH billows ceases. Rather, by the end of the deployment just after 0002 UTC, a single larger (~1 km) wide area of inferred horizontal vorticity O~10^{-1} s^{-1} develops and is centered just below 3 km AGL, perhaps consistent with the sense of a strengthening baroclinic solenoid (Fig. 5).

4. DESCENDING REFLECTIVITY CORE CASE – 25 MAY 2010, TRIBUNE, KS

The 25 May 2010 VORTEX2 case featured the development of a weak (EF0) tornado associated with a supercell thunderstorm near Tribune, KS. Details of these tornadoes are discussed by Tanamachi et al. (2013).

TTUKa-2 began its deployment at 2258 UTC, approximately 20 minutes prior to tornadogenesis. PPI scans (not shown) document the strengthening of inferred vertical vorticity within the developing hook echo. At 2307, the PPI scans were aborted in favor of a sequence of RHI scans across the hook region (Fig. 6). This period, from 2307-2312 UTC, runs up to five minutes prior to the genesis of the tornado northwest of Tribune, KS. As such, the cross section allows us a look at the region through which air parcels are traveling, inbound to the low-level mesocyclone as the tornado develops. Vertical vorticity, estimated from SMART-R radial velocity data, increases sharply following the conclusion of these RHI scans (Fig. 7) over the upstream portion of the hook echo.

A series of descending reflectivity cores is obvious in the time series of RHIs over the period of observation. The motion of the first core is quite discontinuous, rapidly descending from 2.75 km AGL to 1.25 km AGL in the 2309:06 to 2309:47 UTC period (approximately 35 m s^{-1}; Fig. 8). A similar subsequent jump was noted from 2310:00 to 2310:43 UTC, with the core descending from 1.25 km AGL to 750 m AGL. Concurrently, at 2310:00 UTC, another local maximum in reflectivity based at 3 km AGL descends completely to the surface over the span of the next 80 s (approximately 35-40 m s^{-1}; Fig. 9). Yet another core, based at 4 km AGL, descends at roughly the same rate through this same period. (RHI scans terminate at 2311:37 before it impacts the surface.) Over this period, SMART-R 0.7 deg PPIs, centered at ~250 m AGL over the hook region, show a sharp increase in isolated reflectivity maxima within the developing hook body (Fig. 6), likely the identification of these same descending cores.

A significant signature in radial velocity is evident attendant to, particularly, the second set of descending cores. Horizontal vorticity (using (1); no correction is made for fall velocity) is calculated to be approximately .06 s^{-1} along the inside (northeast side) of these descending channels (Fig. 10), much akin to the notion of the vortex rings illustrated by Markowski and Richardson (2008). Beyond these local areas of intense horizontal vorticity, over the period 2310:56 to 2311:37 UTC there is a clear decrease in outbound velocity along the ϕ=10-15 deg radials,

within these descending channels and their wake (Fig. 11). Though it is impossible with single-Doppler RHI data to map these trends singularly to vertical velocity, there is quite likely an increase in the magnitude of horizontal vorticity within the lowest 2.5 km of the hook region through the final 30 s of the deployment, five minutes prior to tornadogenesis.

6. SUMMARY AND DISCUSSION

This study considers observations of horizontal vorticity maxima within the hook echo and along the RFGF of two supercell thunderstorms, afforded by the high-frequency (35 GHz) TTUKa band radars. Both cases are from the 2010 field phase of the VORTEX2 Project.

For the 12 May 2010 case, RHIs were performed roughly east-to-west across the apex of the RFGF as it surged northward. The structure of the boundary very much resembled a density current within the lowest 2 km AGL, sharply sloping rearward with height. However, above 2 km AGL, a clear boundary also exists that tilts forward (eastward) with height, subsequently inflects, discontinuously propagates eastward, and develops a number of KH billows that ascend quickly up the interface. The period of billow activity begins just as the RFGF crosses through the RHI plane, and ceases quickly afterwards as the forward portion of the boundary slope transitions into a uniform front-to-rear slope over the entire lowest 5 km AGL. A much larger (~1 km) horizontal circulation becomes apparent at this time as well, consistent with the sense of a baroclinic mechanism.

The presence of a forward-tilted boundary is somewhat surprising in this context, and calls into question what the reflectivity fineline above 2 km AGL actually represents. It is likely *not* the leading edge of attenuated precipitation, as the reflectivity gradient is not particularly strong, there is a collocated confluent signal in radial velocity, and KH billows develop along this inflecting boundary. The boundary is also not the edge of an updraft as the sense of vorticity (pointing south) is incorrect. Rather, strong increases in radial velocity behind (west of) the boundary at the point of inflection and billow generation suggest there is likely the presence of downdraft air that happens to be overhanging the surface density current structure. More study is certainly necessary to understand the causes of this feature. Naturally, any sources of horizontal vorticity in the storm-scale supercell environment draw attention for the potential relevance to the low- or mid-level mesocyclone vorticity budget. It is impossible in this study to attribute any meaning in that regard.

The 25 May 2010 case provided a detailed look at DRCs within the hook echo region of a weakly tornadic supercell near Tribune, KS. In total, three separate cores are observed to rapidly descend at 35-40 m s^{-1} and inferred horizontal voriticity on the inside (northeast) portion of these descending channels is O~10^{-1} s^{-1}. This sense of vorticity is consistent with the notion of descending baroclinically generated vortex rings (e.g., as illustrated by Markowski and Richardson (2008)), with the understanding that these rings will approach the surface, then be tilted and stretched by the primary updraft.

The compelling factor in this case is that the RHI cross sections were taken through the rear portion of the hook approximately five minutes prior to tornadogenesis. As such, given the advective time scale for this case and the prior knowledge of trajectory patterns through the hook region en route to the low-level mesocyclone (e.g., Klemp and Rotunno 1983; Wicker and Wilhelmson 1995; Beck and Weiss 2013; Dahl et al. 2013), there is a high likelihood that the TTUKa is sampling some of the parcels that ultimately contribute to the evolution of low-level vertical vorticity near tornadogenesis time. With this in mind, beyond the horizontal vorticity directly on the fringes of the descending cores, there appears to be a larger sense of increase in horizontal vorticity across a 1-km expanse of the hook as the RHI scans end, which may be relevant to the increase in low-level vertical vorticity downstream at the time of tornadogenesis.

7. ACKNOWLEDGEMENTS

This study is funded by NSF grant AGS-0800542 and AGS-0964088. Many thanks to the faculty and students within the Texas Tech Atmospheric Science Group and the Wind Science Engineering and Research Center for their time and talents during the VORTEX2 field phase. Thanks also to Josh Wurman, Karen Kosiba and Rachel Humphrey (DOWs); and Mike Biggerstaff and Lou Wicker (SMART-Rs) for collecting and providing the mobile radar data used in this study.

8. REFERENCES

Adlerman, E. J., K. K. Droegemeier, and R. Davies-Jones, 1999: A numerical simulation of cyclic mesocyclogenesis, *J. Atmos. Sci.,* **56**, 2045-2069.

Beck, J. R., and C. C. Weiss, 2013: An assessment of low-level baroclinity and vorticity within a simulated supercell. *Mon. Wea. Rev.*, **141**, 649-669.

Byko, Z., P. Markowski, Y. Richardson, J. Wurman, and E. Adlerman, 2009: Descending reflectivity cores in supercell thunderstorms observed by mobile radars and in a high-resolution numerical simulation. *Wea. Forecasting*, **24**, 155-186.

Dahl, J. M. L., M. D. Parker, and L. J. Wicker, 2013: Imported and storm-generated near-ground vertical vorticity in a simulated supercell. *J. Atmos. Sci*. (submitted)

Davies-Jones, R. P., 2000: A Lagrangian model for baroclinic genesis of mesoscale vortices. Part I: Theory. *J. Atmos. Sci.*, **57**, 715-736.

Davies-Jones, R. P., and H. E. Brooks, 1993: Mesocyclogenesis from a theoretical perspective. *The Tornado: Its Structure, Dynamics, Prediction, ad Hazards. Geophys. Monogr.*, Vol. 79, Amer. Geophys. Union, 105-114.

Kennedy, A., J. M. Straka, and E. N. Rasmussen, 2007: A statistical study of the association of DRCs with supercells and tornadoes. *Wea. Forecasting*, **22**, 1191-1199.

Klemp, J. B., and R. Rotunno, 1983: A study of the tornadic region within a supercell thunderstorm. *J. Atmos. Sci.*, **40**, 359-377.

Markowski, P. M., Y. Richardson, E. Rasmussen, J. Straka, R. Davies-Jones, and R. J. Trapp, 2008: Vortex lines within low-level mesocyclones obtained from pseudo-dual-Doppler radar observations. *Mon. Wea. Rev.*, **136**, 3513-3535.

Markowski, P. M., Y. Richardson, J. Marquis, R. Davies-Jones, J. Wurman, K. Kosiba, P. Robinson, E. Rasmussen, D. Dowell, 2012a: The pretornadic phase of the Goshen County, Wyoming, supercell of 5 June 2009 intercepted by VORTE2. Part I: Evolution of kinematic and surface thermodynamic fields. *Mon. Wea. Rev.*, **140**, 2887-2915.

Markowski, P. M., Y. Richardson, J. Marquis, R. Davies-Jones, J. Wurman, K. Kosiba, P. Robinson, E. Rasmussen, D. Dowell, 2012b: The pretornadic phase of the Goshen County, Wyoming, supercell of 5 June 2009 intercepted by VORTE2. Part II: Intensification of low-level rotation. *Mon. Wea. Rev.*, **140**, 2916-2938.

Rasmussen, E. N., J. M. Straka, M. S. Gilmore, R. Davies-Jones, 2006: A preliminary survey of rear-flank descending reflectivity cores in supercell storms. *Wea. Forecasting*, **21**, 923-938.

Rotunno, R. and J. Klemp, 1985: On the rotation and propagation of simulated supercell thunderstorms. *J. Atmos. Sci.*, **42**, 271-292.

Tanamachi, R. L, H. B. Bluestein, M. Xue, W.-C. Lee, K. A. Orzel, S. J. Frasier, and R. M. Wakimoto, 2013: Near-surface vortex structure in a tornado and in a sub-tornado-strength, convective-storm vortex observed by a mobile, W-band radar during VORTEX2. *Mon. Wea. Rev.* (in press).

Weiss, C. C., J. L. Schroeder, J. Guynes, A. E. Reinhart, P. S. Skinner, and S. Gunter, 2011: A Review of Texas Tech Ka-band operations during VORTEX2. *Preprints, 35th Conference on Radar Meteorology,* Pittsburgh, PA, paper 7B.2

Wicker, L. J., and R. B. Wilhelmson, 1995: Simulation and analysis of tornado development and decay within a three-dimensional supercell thunderstorm. *J. Atmos. Sci.*, **52**, 2675-2703.

Figure 1 – Photographs of an HP supercell near Willow, OK at (left, to southwest) 0001:51 and (right, to west) 0001:47 UTC, during the TTUKa RHI scans. These photos were taken from a location separate from the TTUKa by the LSC/NCAR Photogrammetry Team (Atkins, Wakimoto, Lee).

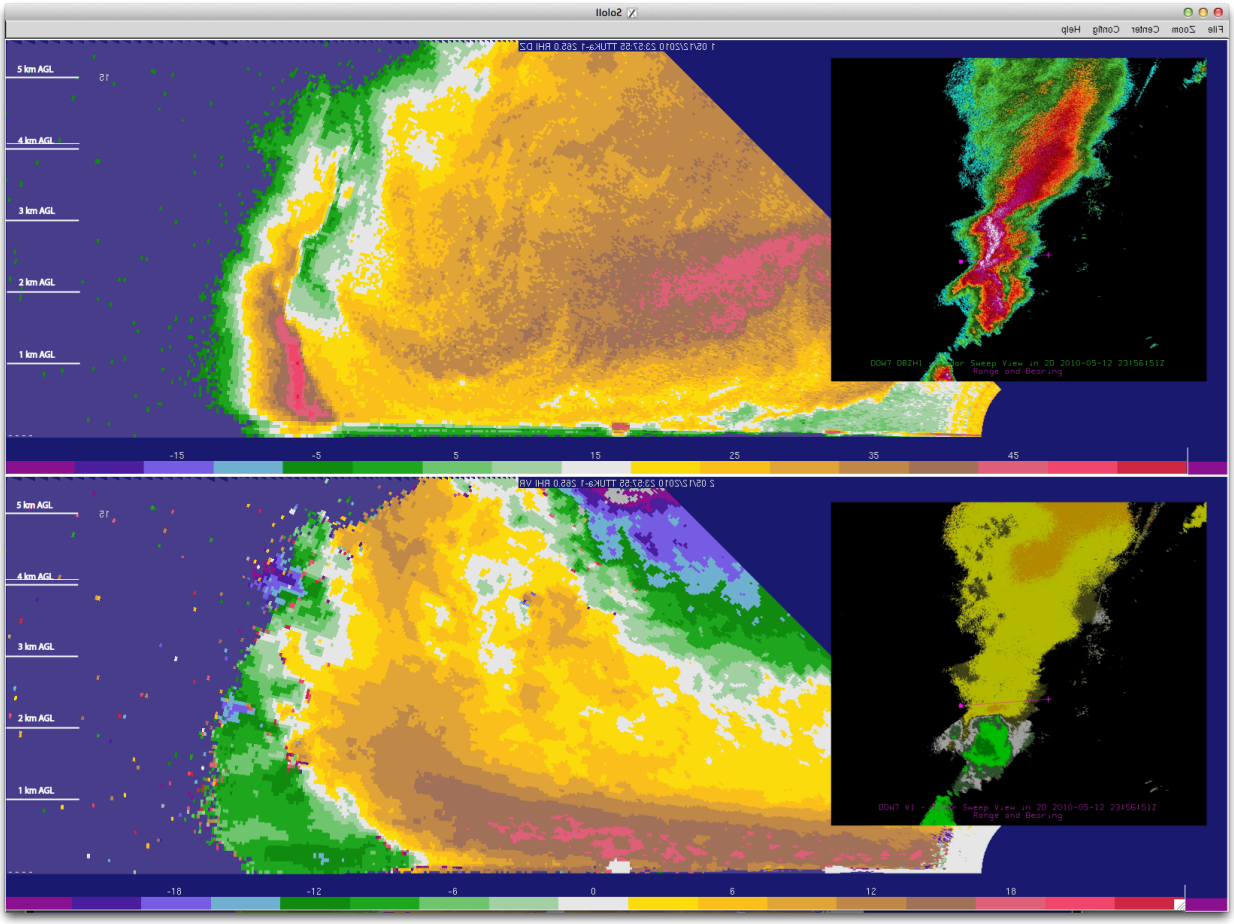

Figure 2 – TTUKa RHI (top) reflectivity (dBZ) and (bottom) radial velocity (m s^{-1}) valid at 2358:15 UTC on 12 May 2010, near Willow, OK. Inset to the right are DOW7 (top) reflectivity and (bottom) radial velocity from a 0.5 deg surveillance scan valid at 2356:51 UTC. The purple line in the inset is the plane of the TTUKa RHI cross section. TTUKa reflectivity and radial velocity scales are provided, as well as an altitude scale.

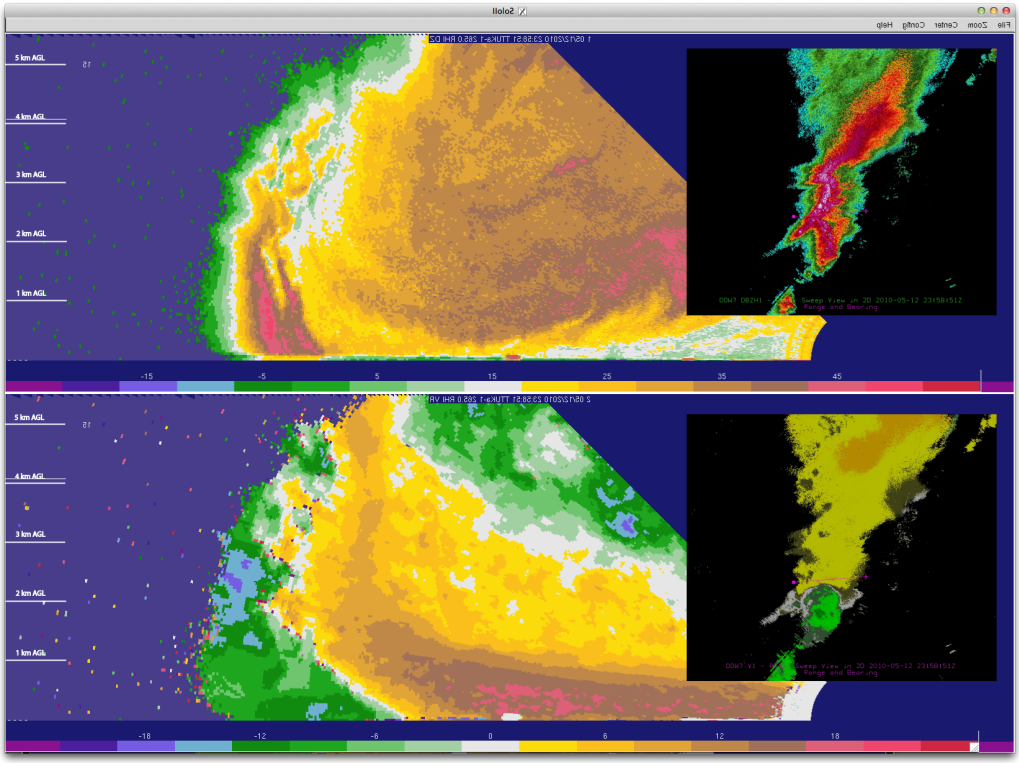

Figure 3 – Same as Fig. 2, but valid at 2358:51 UTC

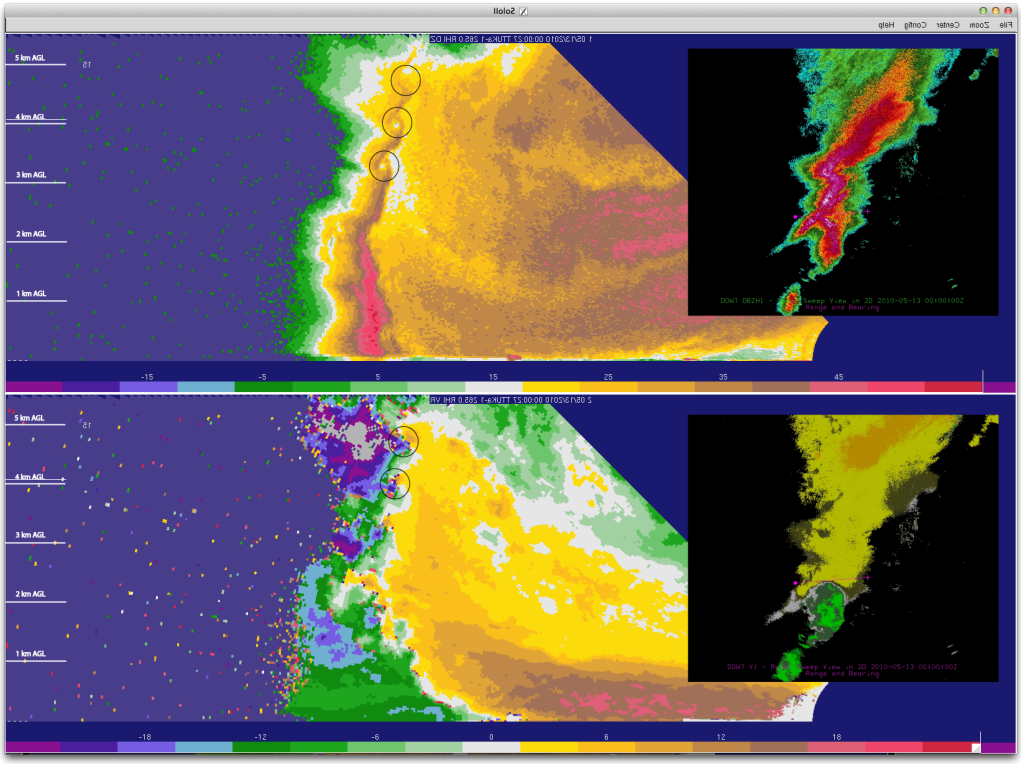

Figure 4 – Same as Fig. 2, but valid at 0000:27 UTC (13 May 2010). Black circles indicate the position of KH billows, referred to in the text.

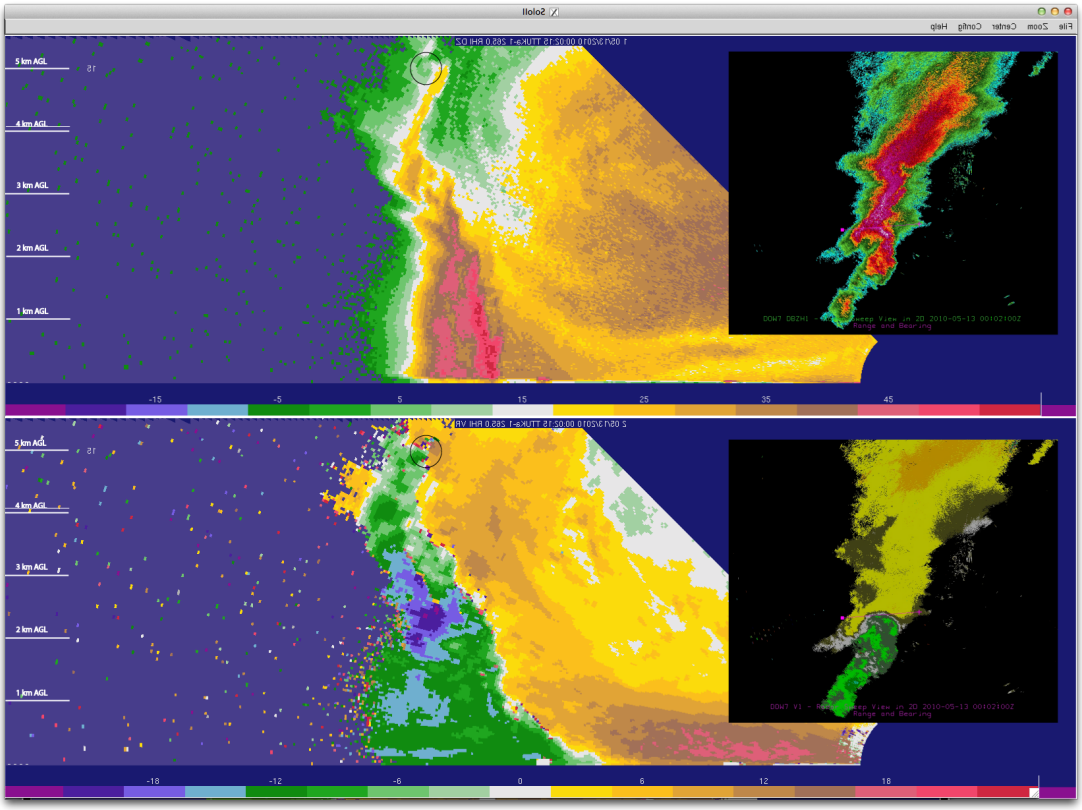

Figure 5 – Same as Fig. 2, but valid at 0002:15 UTC (13 May 2010). Black circles indicate the position of KH billows, referred to in the text.

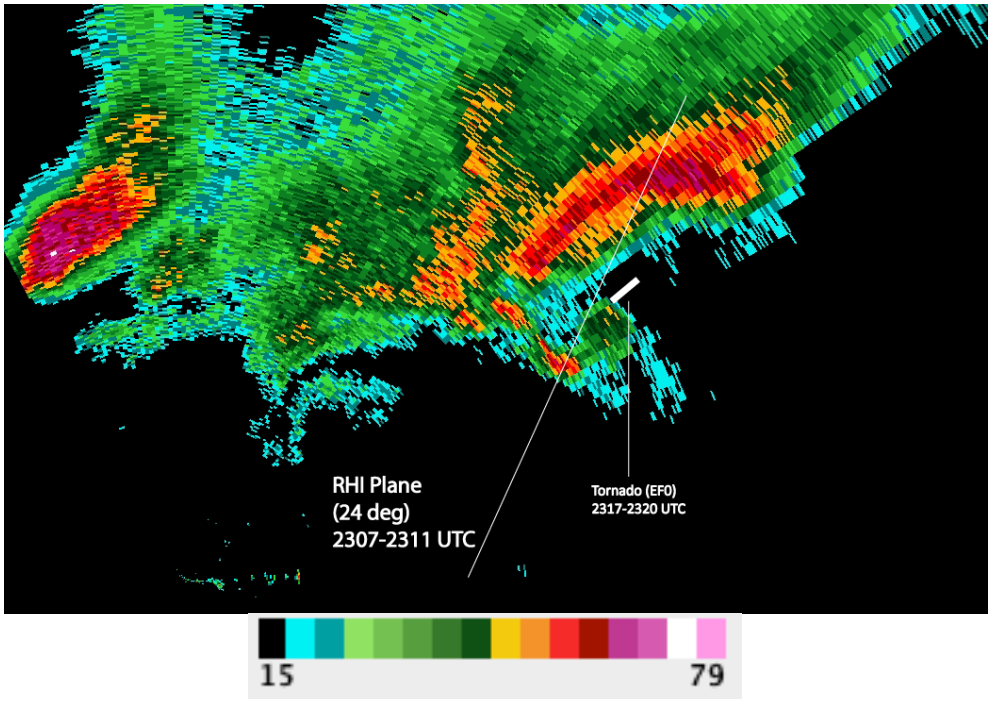

Figure 6 – SMART-R2 0.7 deg reflectivity (dBZ), valid at 2312:41 UTC on 25 May 2010. The angled thin white line denotes the plane of the TTUKa RHI section. The bold white line indicates the tornado path from 2317-2320 UTC.

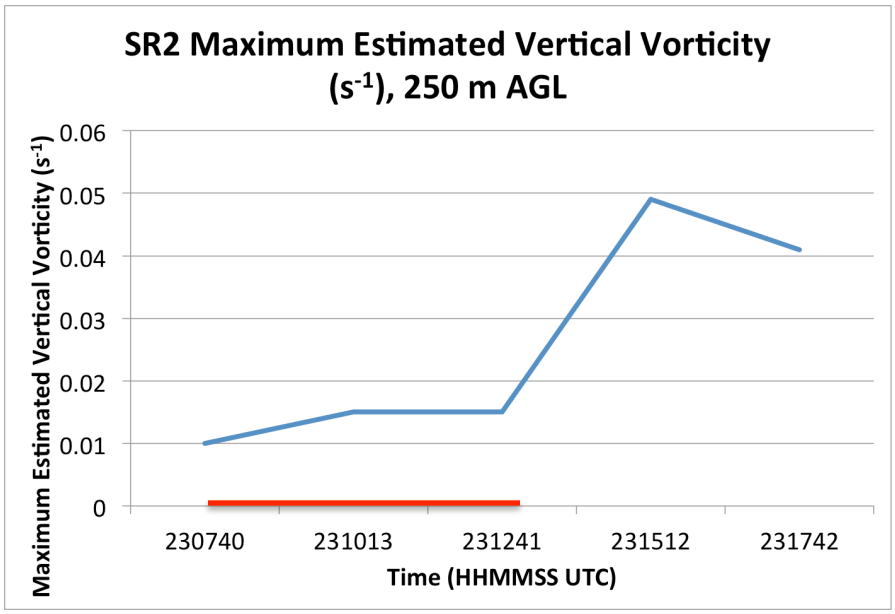

Figure 7 – Estimated maximum 250 m AGL vertical vorticity (s^{-1}) from SMART-R2 radial velocity measurements. The red line denotes the period over which TTUKa RHIs were performed across the hook.

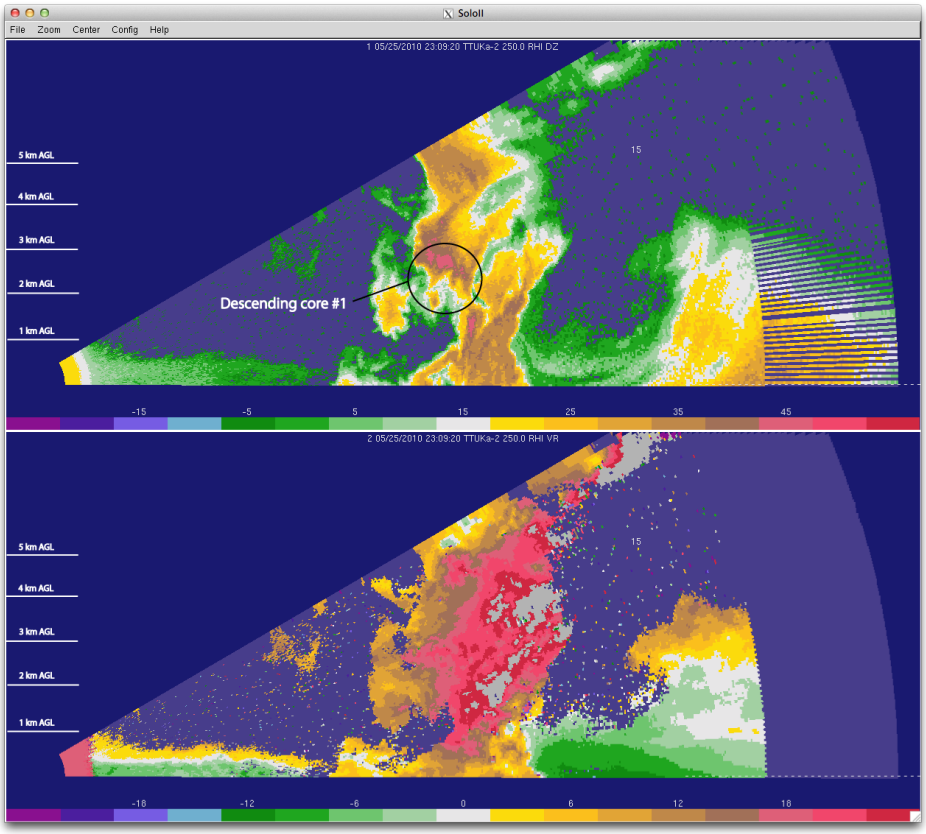

Figure 8 – TTUKa RHI (top) reflectivity (dBZ) and (bottom) radial velocity (m s^{-1}) valid at 2309:20 UTC on 25 May 2010 near Tribune, KS. The location of the first DRC is highlighted. TTUKa reflectivity and radial velocity scales are provided, as well as an altitude scale.

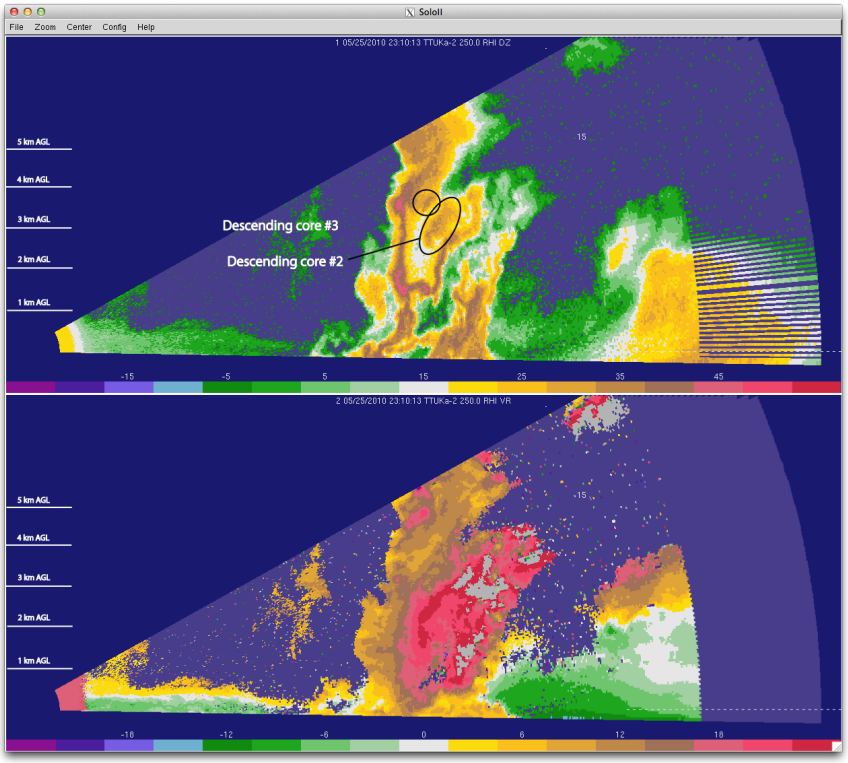

Figure 9 – Same as Fig. 8, but valid at 2310:13 UTC. The locations of the second and third DRCs are highlighted.

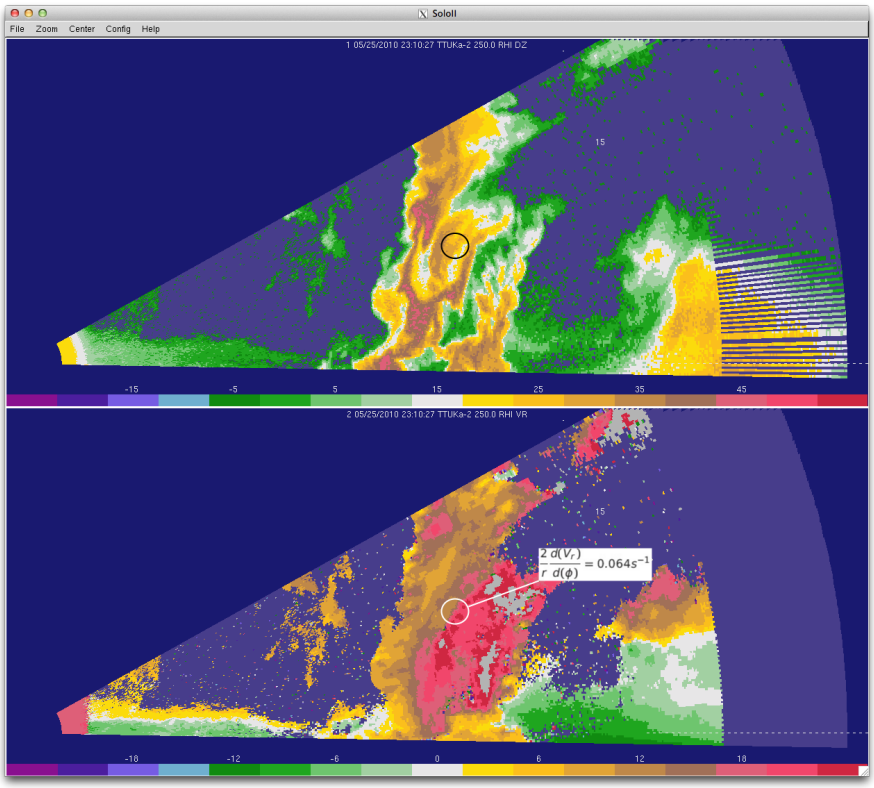

Figure 10 – Same as Fig. 8, but valid at 2310:27 UTC. The location of the horizontal vorticity calculation referred to in the text is indicated.

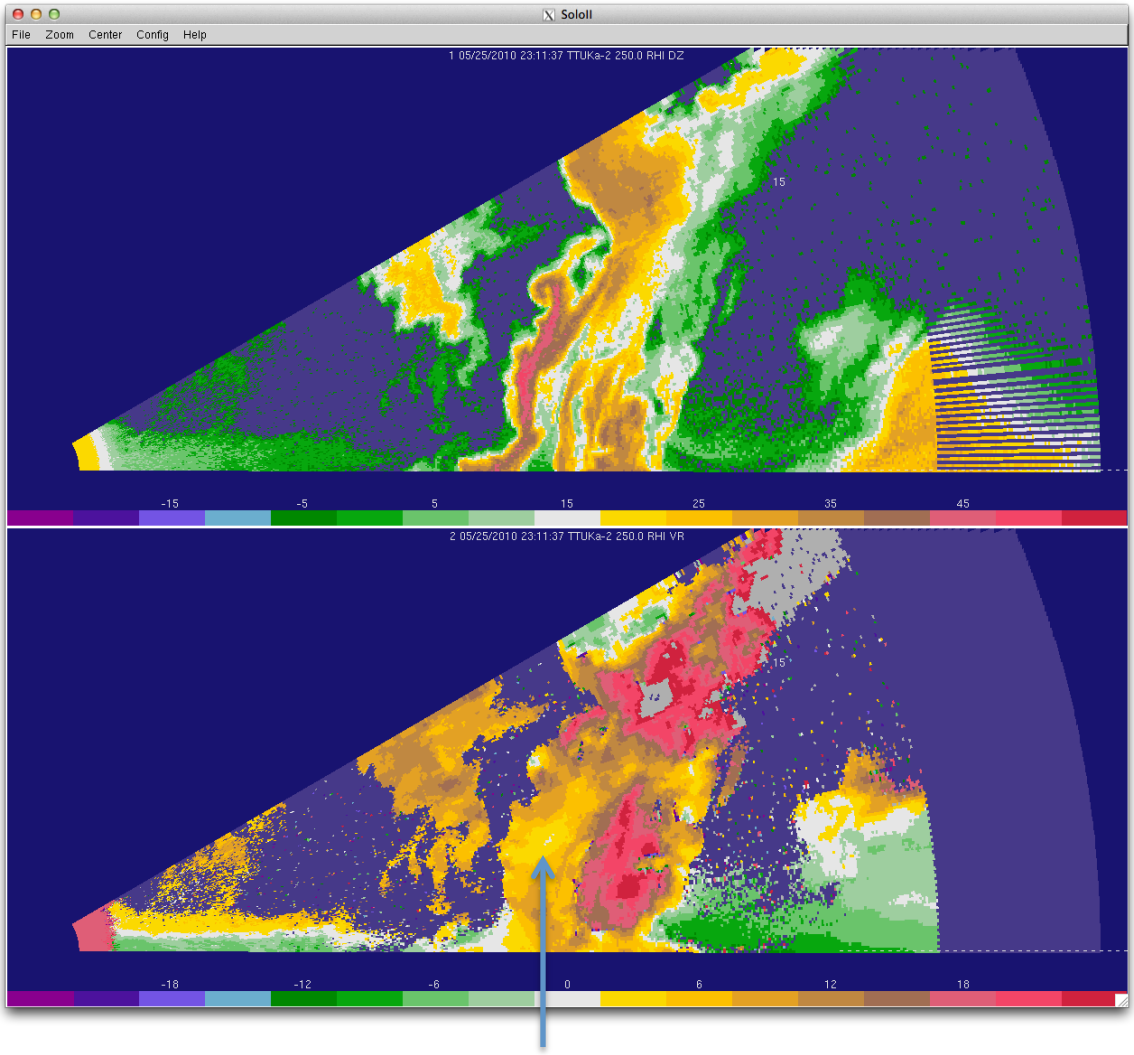

Figure 11 – Same as Fig. 8, but valid at 2311:37 UTC. The location of markedly decreased outbound velocity in the wake of the second and third DRC is indicated by the arrow.